



Molecular Crystals and Liquid Crystals Science and Technology. Section A. Molecular Crystals and Liquid Crystals

Publication details, including instructions for authors and subscription information:

<http://www.tandfonline.com/loi/gmcl19>

DETERMINATION OF MOLECULAR PARAMETERS OF THE MHPB(H)PBC AND MHPB(F)PBC ANTIFERROELECTRIC LIQUID CRYSTALS

Z. Raszewski ^a, J. Kedzierski ^a, J. Kutkowska ^a,
 W. Piecek ^a, P. Perkowski ^b, K. Czupryński ^a, R.
 Dabrowski ^a, W. Drzewiński ^a, J. Zieliński ^a & J.
 Zmija ^a

^a Military University of Technology, 00-908,
 Warsaw, POLAND

^b Graduate School of Engineering, Tohoku
 University, Aoba 05, Aramaki, Aoba-Ku, Sendai,
 980-8579, JAPAN

Version of record first published: 24 Sep 2006

To cite this article: Z. Raszewski, J. Kedzierski, J. Kutkowska, W. Piecek, P. Perkowski, K. Czupryński, R. Dabrowski, W. Drzewiński, J. Zieliński & J. Zmija (2001): DETERMINATION OF MOLECULAR PARAMETERS OF THE MHPB(H)PBC AND MHPB(F)PBC ANTIFERROELECTRIC LIQUID CRYSTALS, *Molecular Crystals and Liquid*

To link to this article: <http://dx.doi.org/10.1080/10587250108024001>

PLEASE SCROLL DOWN FOR ARTICLE

Full terms and conditions of use: <http://www.tandfonline.com/page/terms-and-conditions>

This article may be used for research, teaching, and private study purposes. Any substantial or systematic reproduction, redistribution, reselling, loan, sub-licensing, systematic supply, or distribution in any form to anyone is expressly forbidden.

The publisher does not give any warranty express or implied or make any representation that the contents will be complete or accurate or up to date. The accuracy of any instructions, formulae, and drug doses should be independently verified with primary sources. The publisher shall not be liable for any loss, actions, claims, proceedings, demand, or costs or damages whatsoever or howsoever caused arising directly or indirectly in connection with or arising out of the use of this material.

Determination of Molecular Parameters of the MHPB(H)PBC and MHPB(F)PBC Antiferroelectric Liquid Crystals

Z. RASZEWSKI^a, J. KEDZIERSKI^a, J. RUTKOWSKA^a, W. PIECEK^a,
P. PERKOWSKI^b, K. CZUPRYŃSKI^a, R. DĄBROWSKI^a,
W. DRZEWIŃSKI^a, J. ZIELIŃSKI^a and J. ŻMIJA^a

^a*Military University of Technology, 00-908 Warsaw, POLAND and* ^b*Graduate
School of Engineering, Tohoku University, Aoba 05, Aramaki, Aoba-Ku, Sendai
980-8579 JAPAN*

Two investigated antiferroelectric liquid crystals, MHPB(H)PBC and MHPB(F)PBC, were synthesized [1] and some their physical properties were described earlier [2]. Apart of the above, MHPB(H)PBC and MHPB(F)PBC have been studied by means of dielectric, densitometric, refractometric and X-ray measurements. Spontaneous polarization P_s and tilt angle θ in ferro- (SmC*) and antiferroelectric (SmC_A*) phases of MHPB(H)PBC and MHPB(F)PBC have also been investigated. Transverse α_t and longitudinal α_l molecular polarizabilities have been calculated from the ordinary n_o and extraordinary n_e refractive indices and density ρ of MHPB(H)PBC and MHPB(F)PBC, using Neugebauer's, Vuks and Lorentz equations with both Haller and Subramanyama extrapolation procedures. Effective values of the molecular dipole moment μ have been calculated from electric permittivity ϵ in the I phases of these compounds, using Maier and Meier equation.

Keywords: antiferroelectric liquid crystals; dipole moment; transverse and longitudinal molecular polarizabilities

INTRODUCTION

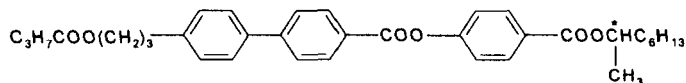
Since the discovery of the antiferroelectric SmC_A^* phase [3], a variety of theoretical and experimental investigations have been performed, in order to understand its origin and nature. In 1997, two antiferroelectric liquid crystals, MHPB(H)PBC and MHPB(F)PBC, were synthesized at the Military University of Technology in Warsaw [1]. The MHPB(H)PBC antiferroelectric is characterized by direct transition from the smectic SmA^* phase to the ferroelectric smectic SmC_A^* phase, while MHPB(F)PBC exhibits the ferroelectric phase SmC^* between paraelectric SmA^* and antiferroelectric SmC_A^* ones. Preliminary studies of these antiferroelectric materials, performed by our team [1], as well as results reported in [2], show without doubt that substitution of the terminal group $-\text{C}_3\text{F}_7$ in MHPB(F)PBC in the place of $-\text{C}_3\text{H}_7$ in MHPB(H)PBC results not only in the appearance of the SmC^* phase between SmA^* and SmC_A^* ones, but also in increase (by about four times) of spontaneous polarization P_s of the smectic SmC_A^* layer of the MHPB(F)PBC, as compared to P_s observed in the smectic SmC_A^* layer of the MHPB(H)PBC.

The aim of this work was to determine molecular parameters of two above-mentioned analogues, with such small difference between corresponding molecular structures. As substitution of the $-\text{C}_3\text{F}_7$ terminal group instead of the $-\text{C}_3\text{H}_7$ one only slightly affects spatial structure of the molecule, authors expected that changes of molecular parameters determined in this paper that result from this substitution should, to a certain degree, be reflected in ferro- and antiferroelectric smectic phases sequence of these liquid crystals.

EXPERIMENTAL

Two following compounds have been selected as the antiferroelectric liquid crystals for study:

[44- (1-methylheptyloxycarbonyl)phenyl]-4'-[3-(butanoiloxy)prop-1-oxy]biphenyl carboxylate (in short) MHPB(H)PBC

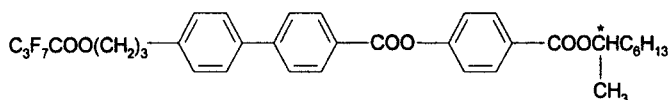


with the phase sequence:

Cr 67.0 Sm I_A*(43,0)Sm C_A* 92,8 Sm A*116,2 I, and

4-[4(1-methylheptyloxycarbonyl)phenyl]-4'-[3-(2,2,3,3,4,4,4-heptafluorobutanoiloxy) prop-1-oxy]biphenyl carboxylate (in short)

MHPB(F)PBC



with the phase sequence:

Cr83,5Sm I_A*(54,0)Sm C_A*121,0Sm C*123,6Sm A*128,8 I

Table 1 shows transition temperatures and enthalpies for MHPB(H)PBC and MHPB(F)PBC. The phase transition temperatures and enthalpies have been determined by differential scanning calorimetry (DSC), using the SETARAM 92 calorimeter. Liquid crystal transition temperatures and phase textures have also been observed, using the BIOLAR PI microscope equipped with the LINKAM 660 hot stage, controlled by the TMS 93 unit.

TABLE 1. Transition temperatures T_D [°C] and enthalpies ΔH [kJ/mol], determined by DSC, and transition temperatures T_M [°C] determined by optical microscopy for MHPB(H)PBC and MHPB(F)PBC

		SmI _A *	SmC _A *	SmA*	I
MHPB(H)PBC	T_D	-	92.8	116.2	
	ΔH	-	0.13	5.25	
	T_H	43.0	93.0	116.6	
		SmC _A *	SmC*	SmA*	I
MHPB(F)PBC	T_D	121.0	123.6	128.8	
	ΔH	0.12	1.37	3.73	
	T_H	121.0	123.8	129.0	

These compounds have been studied using electrooptical, dielectric, densitometric, refractometric and microscopic methods. All measurements have been performed while cooling from the isotropic phases, the cooling rate being 0.01 deg/min.

Tilt angle

Tilt angles θ have been studied by means of optical switching angle measurement and X-ray methods [5]. Figures 1 and 2 show the tilt angle vs. temperature for MHPB(H)PBC and MHPB(F)PBC, respectively. It is interesting to note that, in spite of the fact that ΔH values (given in Table 1) shows the phase transition $\text{SmC}^* \rightarrow \text{SmC}_A^*$ of the fluorinated compound to be rather of the first order type, Fig.1 nevertheless reveals pronounced step of the tilt angle value for this phase change.

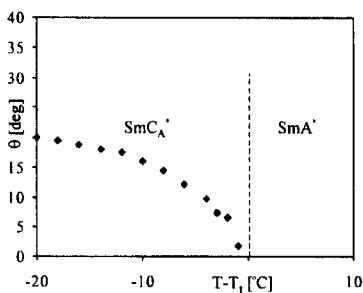


FIGURE 1. Tilt angle θ vs. temperature for MHPB(H)PBC

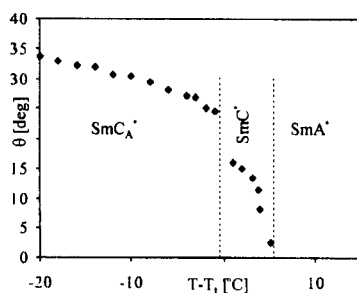


FIGURE 2. Tilt angle θ vs. temperature for MHPB(F)PBC

Our results for both materials in their antiferroelectric SmC_A^* phases are nearly the same as those reported in [2] and [6].

Spontaneous polarization

Spontaneous polarization P_s has been measured by means of the Diamant bridge method and pulse technique. Both these measurements have been performed on the same sample, using commercially available Linkam cells or cells specially prepared for this purpose. The cell spacing was measured directly, using the interference method, for each sample and was kept between 5 and 7 μm . Cells were filled with the isotropic phase of the studied substance and then the samples were

slowly cooled from the isotropic phase to smectic phases in the presence of low frequency AC electric field. During the alignment process and measurements, temperature was controlled with the Linkam TSM 92 hot stage. Results of these measurements are shown in Figs.3 and 4.

Our results from the A-C bridge and pulse experiments are in good agreement with each other, as well as with data for SmC_A^* phases reported in [2].

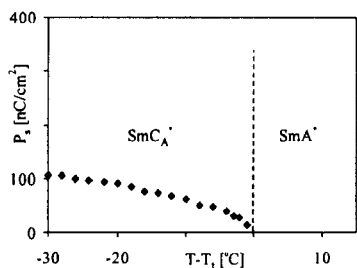


FIGURE 3. Spontaneous polarization P_s vs. temperature for MHPB(H)PBC

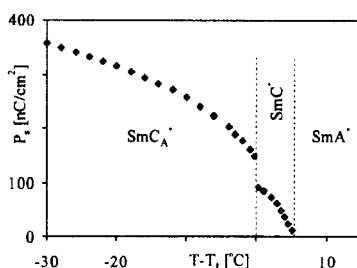


FIGURE 4. Spontaneous polarization P_s vs. temperature for MHPB(F)PBC

Since the spontaneous polarization P_s of tilted smectic layer is directly proportional to molecular density number N , effective permanent molecular dipole moment μ and tilt angle θ [4]

$$P_s \sim N\mu \sin \theta$$

the P_s jump at the transition from SmC^* to SmC_A^* in MHPB(F)PBC is a natural consequence of the θ jump at this transition. Pronounced P_s increase in the SmC_A^* phase of the fluorinated compound, as compared to the non-fluorinated one, can also, to a first approximation, be explained by a marked increase of θ accompanying the substitution of the $-\text{C}_3\text{F}_7$ terminal group instead of the $-\text{C}_3\text{H}_7$ one. The above is correct as N (which is directly proportional to the density ρ) remains continuous at this transition, which can be seen from Figure 6.

Density

Density ρ has been measured by means of the Paar densitometer DMA 46 with DMA 602 measuring cell, in the I, SmA^* , SmC^* and SmC_A^*

phases. Densities as functions of temperature for MHPB(H)PBC and MHPB(F)PBC are shown in Figs.5 and 6, respectively.

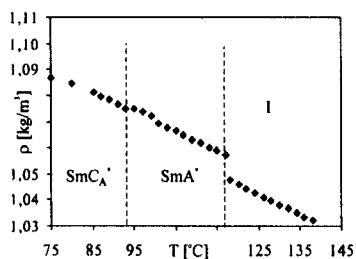


FIGURE 5. Temperature dependence of density ρ for the I, SmA^* and SmCA^* phases of MHPB(H)PBC

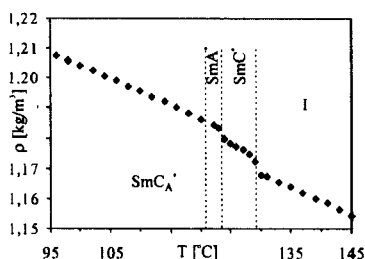


FIGURE 6. Temperature dependence of density ρ for the I, SmA^* , SmC^* and SmCA^* phases of MHPB(F)PBC

It is worth to point out that density ρ remains continuous at the $\text{SmC}^* \rightarrow \text{SmCA}^*$ transition of MHPB(F)PBC, while the $\text{SmA}^* \rightarrow \text{SmCA}^*$ transition of MHPB(H)PBC is accompanied by only a slight density decrease.

Refractive indices

The refractive indices: isotropic n_i , ordinary n_o and extraordinary n_e have been measured using combined methods, applying both appropriately prepared Abbe refractometer and interference wedge. Values of the $n_{\perp}(T)$, $n_i(T)$ and $n_{\parallel}(T)$ are presented graphically in Figs.7 and 8.

Please note that refractive indices $n_{\perp}(T)$ and $n_{\parallel}(T)$, shown in Figs.7 and 8 for the SmA^* , SmC^* and SmCA^* phases are related to the optical axis perpendicular to the smectic planes. In the SmA^* phase the above-mentioned axis coincides with the molecular director \mathbf{n} of SmA^* smectic layers, while in the SmCA^* phase this direction is determined by the helical axis of this phase.

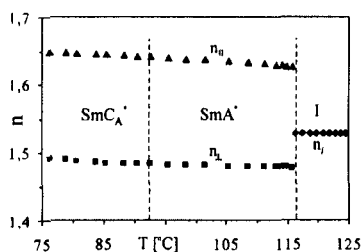


FIGURE 7. Temperature dependence of the $n_{\perp}(T)$, $n_{\parallel}(T)$ and $n_i(T)$ refractive indices for MHPB(H)PBC

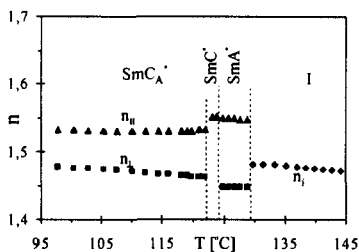


FIGURE 8. Temperature dependence of the $n_{\perp}(T)$, $n_{\parallel}(T)$ and $n_i(T)$ refractive indices for MHPB(F)PBC

Electric permittivities.

Dielectric properties of the MHPB(H)PBC and MHPB(F)PBC have been studied in the I, SmA*, SmC* and SmC_A* phases over the frequency range from 10 Hz to 10 kHz, using HP6425 amplitude analyzer. Dielectric measurements have been performed with the same samples as used for spontaneous polarization measurements. Temperature dependence of the perpendicular component ϵ_{\perp} of the electric permittivity ϵ real part for both compounds is shown in Figs.9 and 10.

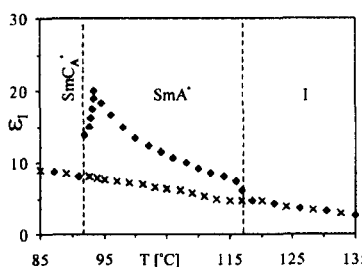


FIGURE 9. Perpendicular component ϵ_{\perp} of the electric permittivity ϵ real part at 100 Hz and 10 kHz for MHPB(H)PBC as a function of temperature.

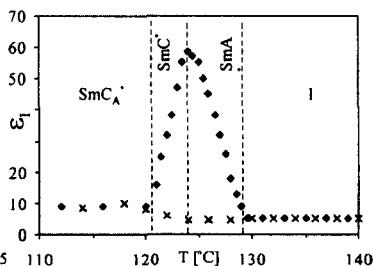


FIGURE 10. Perpendicular component ϵ_{\perp} of the electric permittivity ϵ real part at 100 Hz and 10 kHz for MHPB(F)PBC as a function of temperature.

For both materials, strong soft mode contributions are observed in the SmA* phases. In the SmC* phase of MHPB(F)PBC, Goldstone mode can also be seen.

DISCUSSION

From X-ray investigations we know [5] that length d of objects that produce SmA* phase (thickness of a SmA* layer for MHPB(H)PBC is $d_A(H) = 3.5$ nm and for MHPB(F)PBC is $d_A(F) = 3.3$ nm) is comparable to the corresponding molecule length l (which is $l(H) = 3.4$ nm and $l(F) = 3.5$ nm, as obtained from the Hyper Chem 5.0 code run). This fact may indicate that smectic SmA* phases are made up mainly of monomers or mixture of monomers and dimers of the same lengths.

If we assume that in the course of dimerization electron polarizability is additive and that orientations of dimers and monomers in smectic SmA* layers are described by the same order parameter $S_A(T)$, then we may apply the MSN, CMV and LLC formulae to calculate longitudinal α_l and transverse α_t molecular polarizabilities of molecules under consideration. These formulae:

- (i) – Meier-Saupe, Neugebauer [6],
- (ii) – Chandrasekhar, Madhusudana, Vuks [7],
- (iii) – Lorentz-Lorentz (liquid crystalline) [8]

have been derived for the nematic phase which, from the optical point of view, is uniaxial. It is reasonable, then, to expect that they will also hold for the smectic SmA* phase. Principal refractive indices $n_o(T)$ and $n_e(T)$, which describe optical properties of the smectic SmA* phases (shown in Figs.7 and 8), should thus satisfy the MSN, CMV and LLC formulae.

With experimental data for $n_o(T)$, $n_e(T)$ and $\rho(T)$ for the smectic SmA* phases and $n_l(T)$ and $\rho(T)$ for the isotropic I phases, the MSN, CMV and LLC formulae, together with extrapolation procedures of Haller [7] and Subramanyama [6], have been used to calculate α_l and α_t polarizabilities of MHPB(H)PBC and MHPB(F)PBC molecules. Results for α_l , α_t and $S_A(T)$ are given in Table 2.

As one can see, results for α_l and α_t obtained from the MSN, CMV and LLC formulae are in good agreement with each other. It seems that arithmetic averages (given in the last row of Table 2) of α_l and α_t

values obtained from the MSN, CMV and LLC models may be reasonably taken for further calculations.

Assuming that in the isotropic phase molecules of both substances are not associated, we can estimate effective values of molecular dipole moment μ (on the basis of Maier and Meier equations [9] and dielectric measurement results).

TABLE 2. Results of the α_i , α_t and $S_A(T)$ calculations for MHPB(H)PBC and MHPB(F)PBC

		MHPB(H)PBC				MHPB(F)PBC			
		$\alpha_t \cdot 10^{39}$	$\alpha_i \cdot 10^{39}$	$\alpha \cdot 10^{39}$	S_A	$\alpha_t \cdot 10^{39}$	$\alpha_i \cdot 10^{39}$	$\alpha \cdot 10^{39}$	S_A
MSN	*	9.43	6.15	7.24	0.81	9.00	6.54	7.36	0.86
	**	9.41	6.16	7.24	0.82	9.00	6.54	7.36	0.86
CMV	*	9.04	6.34	7.24	0.89	8.57	6.75	7.36	0.90
	**	9.07	6.32	7.24	0.91	8.59	6.74	7.36	0.92
LLC	*	8.42	6.65	7.24	0.93	8.21	6.94	7.36	0.92
	**	8.45	6.63	7.24	0.90	8.22	6.93	7.36	0.90
		8.97	6.38	7.24		8.60	6.74	7.30	

S_A – molecular order parameter of the SmA* phase at $T - T_i = -4^\circ\text{C}$

α in $[\text{C}^2\text{m}^2\text{J}^{-1}]$

* - results obtained with the Haller extrapolation procedure

** - results obtained with the Subramanyama extrapolation procedure

With temperature characteristics $\rho(T)$ and $\varepsilon(T)$ for the isotropic phase known, and using previously estimated α_t and α_i values, one can calculate the dipole moment μ by fitting Maier and Meier [9] equation to experimental data. Results of these dielectric calculation are given in Table 3.

TABLE 3. Results of dipole moment calculations for MHPB(H)PBC and MHPB(F)PBC

		MHPB(H)PBC				MHPB(F)PBC			
		$\mu_{\perp}=10^{30}$	$\mu_{\parallel}=10^{30}$	$\mu=10^{30}$	γ	$\mu_{\perp}=10^{30}$	$\mu_{\parallel}=10^{30}$	$\mu=10^{30}$	γ
		C_m	C_m	C_m	deg	C_m	C_m	C_m	deg
*		11±25	4÷6	10.95	5÷6	-	-	11.97	-
**		11.25	4.66	12.15	67.5	11.19	5.89	12.62	62.2

* - results obtained from dielectric measurements,

** - results obtained from computer modeling.

Table 3 lists also dipole moment μ values determined from molecular structure modeling by the ALCHEMY II code. It is worth to point out that our experimental data (obtained from dielectric measurements) are in good agreement with those obtained from computer modeling.

Comparison of molecular parameters μ , μ_{\perp} , α_{\parallel} and α_{\perp} determined in this study for both molecules shows them to differ slightly. It seems that substitution of the $-\text{C}_3\text{F}_7$ terminal group in the place of $-\text{C}_3\text{H}_7$ that results in appearance of the SmC^* ferroelectric phase between paraelectric SmA^* and antiferroelectric SmC_A^* ones is not distinctly reflected in relevant molecular parameters variations, at least to a first approximation. Taking the above into account, together with the fact that hydrogenated and fluorinated molecules have nearly the same molecular structures, we may conclude that the origin of antiferro- and ferroelectricity seems to be very complicated and complex.

Acknowledgments,

This work was supported by the Polish State Committee of Scientific Research under grant No. 7T08A07019.

References

- [1] W. Drzewiński, K. Czupryński, R. Dąbrowski, Z. Raszewski, *SPIE Proc.*, **3319**, 100 (1998).
- [2] A. Fafara, B. Gestblom, S. Wróbel, R. Dąbrowski, W. Drzewiński, D. Kilian, W. Haase, *Ferroelectrics*, **212**, 79 (1998).
- [3] A.D.L. Chandani, E. Górecka, Y. Ouchi, H. Takezoe, A. Fokuda, *Jap. J. Appl. Phys.*, **28**, L1265 (1989).
- [4] Z. Raszewski, J. Kędzierski, P. Perkowski, J. Rutkowska, W. Piecek, J. Zieliński, J. Żmija, R. Dąbrowski, *Mol. Cryst. Liq. Cryst.*, **328**, 255 (1999).
- [5] J. Przedmojski, R. Dąbrowski, K. Czupryński, W. Drzewiński, Will be published in *Biulletin of the MUT* (2000).
- [6] H.S. Subramanyam, C. Praba, D. Krishnamurti, *Mol. Cryst. Liq. Cryst.*, **28**, 201 (1974).
- [7] J. Haller, H.A. Huggins, H.R. Lilienthal, T. Mc Guire, *J. De Phys. Chem.*, **77**, 950, (1973).
- [8] G. Pelzel, *Z. Phys. Chem.*, **255**, 602, (1974).
- [9] W. Maier, G. Meier, *Z. Naturforsch.*, **16a**, 26 (1960).